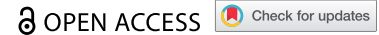


REPORT



Functional GLP-1R antibodies identified from a synthetic GPCR-focused library demonstrate potent blood glucose control

Qiang Liu^a, Pankaj Garg^{a,b}, Burcu Hasdemir^{a,c}, Linya Wang^a, Emily Tuscano^a, Emily Sever^a, Erica Keane^a, Ana G Lujan Hernandez^a, Tom Z. Yuan^a, Eric Kwan^a, Joyce Lai^a, Greg Szot^d, Sreenivasan Paruthiyil^d, Fumiko Axelrod^a, and Aaron K. Sato^a

^aTwist Biopharma, South San Francisco, CA, USA; ^bAlamar Biosciences, Fremont, CA, USA; ^cCatalyst Biosciences, South San Francisco, CA, USA; ^dDiabetes Center, University of California San Francisco, San Francisco, CA, USA

ABSTRACT

G protein-coupled receptors (GPCRs) are a group of seven-transmembrane receptor proteins that have proven to be successful drug targets. Antibodies are becoming an increasingly promising modality to target these receptors due to their unique properties, such as exquisite specificity, long half-life, and fewer side effects, and their improved pharmacokinetic and pharmacodynamic profiles compared to peptides and small molecules, which results from their more favorable biodistribution. To date, there are only two US Food and Drug Administration-approved GPCR antibody drugs, namely erenumab and mogamulizumab, and this highlights the challenges encountered in identifying functional antibodies against GPCRs. Utilizing Twist's precision DNA writing technologies, we have created a GPCR-focused phage display library with 1×10^{10} diversity. Specifically, we mined endogenous GPCR binding ligand and peptide sequences and incorporated these binding motifs into the heavy chain complementarity-determining region 3 in a synthetic antibody library. Glucagon-like peptide-1 receptor (GLP-1 R) is a class B GPCR that acts as the receptor for the incretin GLP-1, which is released to regulate insulin levels in response to food intake. GLP-1 R agonists have been widely used to increase insulin secretion to lower blood glucose levels for the treatment of type 1 and type 2 diabetes, whereas GLP-1 R antagonists have applications in the treatment of severe hypoglycemia associated with bariatric surgery and hyperinsulinemic hypoglycemia. Here we present the discovery and creation of both antagonistic and agonistic GLP-1 R antibodies by panning this GPCR-focused phage display library on a GLP-1 R-overexpressing Chinese hamster ovary cell line and demonstrate their *in vitro* and *in vivo* functional activity.

ARTICLE HISTORY

Received 26 August 2020
Revised 4 February 2021
Accepted 17 February 2021

KEYWORDS


GPCR; glp-1 peptide; phage display library; panning; antagonist; agonist; glucose level

Introduction

G protein-coupled receptors (GPCRs) are an important class of drug targets implicated in a wide range of indications. Of all US Food and Drug Administration (FDA)-approved drugs, around one-third target GPCRs, predominantly comprising small molecules and peptides.^{1–3} Antibodies are large molecules that offer a number of advantages over such molecules due to their binding specificity, much longer serum half-life through FcRn recycling, and limited central nervous system penetration.⁴ It has been very challenging to discover GPCR-targeted antibodies through traditional approaches, due to low expression levels of GPCR proteins on the cell surface, limited extracellular loop surface area, conformational flexibility, and difficulties in generating the purified GPCR proteins in sufficient quantities for use as antigen. The two FDA-approved GPCR-targeting antibodies, mogamulizumab (trade name Poteligeo), which is directed to the CC-chemokine receptor 4 (CCR4) for the treatment of cutaneous T cell lymphoma, and erenumab (trade name Aimovig), which acts on the calcitonin gene-related peptide receptor (CGRP-R) for the treatment of migraine, both target the large N-terminal extracellular domain.⁵

We developed a synthetic antibody phage display library that is focused on GPCRs with the aim of discovering and developing therapeutic antibodies against these difficult targets. Our strategy is unique in that it leverages an in-house commercial silicon-based DNA synthesis platform. This allows synthesis of over 1 million 300 base pair-long oligonucleotides immobilized on a silicon chip, which enables the creation of a new class of synthetic GPCR binding-motif library. This is accomplished by performing a comprehensive, multi-species computational analysis of sequences and structures of all known GPCR ligand interactions, including protein ligands (cytokines, chemokines, viral proteins), peptide ligands (glucagon, gastric inhibitory polypeptide (GIP), glucagon-like peptide (GLP)), peptide mimics, GPCR N-terminal extracellular domains (ECDs), GPCR extracellular loops, and GPCR binding antibodies.^{6,7} Our antibody discovery platform further involves cell-based selections with target over-expressing cell lines presenting the GPCR of interest in a form that is close to its native structure.⁸ The approach allows us to rapidly identify antibodies against multiple GPCRs, and here we present the isolation of antibodies directed to the GPCR glucagon-like peptide-1 receptor (GLP-1 R).

CONTACT Aaron K. Sato  asato@twistbioscience.com  Twist Biopharma, South San Francisco, CA, USA.

 Supplemental data for this article can be accessed on the [publisher's website](#).

© 2021 The Author(s). Published with license by Taylor & Francis Group, LLC.

This is an Open Access article distributed under the terms of the Creative Commons Attribution-NonCommercial License (<http://creativecommons.org/licenses/by-nc/4.0/>), which permits unrestricted non-commercial use, distribution, and reproduction in any medium, provided the original work is properly cited.

GLP-1 R is the receptor for incretin GLP-1 that is released by intestinal L cells (a type of enteroendocrine cell) in response to food intake. GLP-1 is a hormone released primarily from the gastrointestinal tract in response to food intake and controls the secretion of insulin from pancreatic islets in a glucose-dependent manner.^{9,10} GLP-1-induced GLP-1 R activation in pancreatic beta cells results in intracellular signaling that leads to insulin secretion and blood glucose regulation. In vivo, GLP-1 is rapidly inactivated by dipeptidyl peptidase-IV (DPP-4), rendering a biological half-life of less than 5 min.^{9,11} Several GLP-1 peptide agonists based on native sequences have been adapted to improve their pharmacokinetic (PK) properties and are now approved for the treatment of type 2 diabetes. In addition to their insulinotropic action, they can also have beneficial effects on body weight and cardiovascular properties. There are six approved GLP-1 R peptide agonists (analogs of or modified derivatives of GLP-1), namely, exenatide (synthetic exendin-4), liraglutide, lixisenatide, dulaglutide, semaglutide and albiglutide,¹² all of which are formulated for subcutaneous injection and display a longer half-life than GLP-1, mostly due to their resistance to peptidases, such as DPP-IV.¹³ To date, there are no small molecules that targeting the GLP-1 R have been approved for therapeutic purposes, although semaglutide is now also available as an oral preparation.

While the importance of GLP-1 R agonists in targeting hyperglycemia in the context of diabetes therapy is well-established, the role of GLP-1 R antagonism in rectifying hypoglycemia is a rapidly emerging area of biology. Hypoglycemia occurs with varying degrees of severity, is biochemically characterized by the unregulated secretion of insulin from the pancreatic β -cells in the presence of low blood glucose levels and can be caused by several different medical conditions, including congenital and neonatal hyperinsulinism (HI).¹⁴ Congenital HI is a genetic disorder in which the pancreatic beta cells secrete an excess of insulin causing low blood sugar (hypoglycemia). Neonatal HI is a clinical syndrome of pancreatic beta-cell dysfunction characterized by failure to suppress insulin secretion in the presence of hypoglycemia. Whilst rare, HI is the most common cause for persistent hypoglycemia in newborns and children.¹⁵ GLP-1 is a major driver of insulin secretion after bariatric surgery, but post-prandial hypoglycemia can occur in patients following bariatric surgical procedures due to excessive GLP-1 secretion.¹⁶ Since glucose is the main source of fuel for the brain, severe or long-lasting hypoglycemia can cause seizures, unconsciousness, serious brain damage or death. The incidence of congenital HI is ~1 in 40,000 live births in the general population and ~60% of infants with this condition experience a hypoglycemic episode within the first month of life, thus increasing the risk of serious complications. Unlike hypoglycemia that occurs after fasting or exercising in healthy people, patients with HI can experience episodes of hypoglycemia after eating. HI is a condition that can overlap with various metabolic conditions, many of which are interlinked due to disease progression/severity. For example, obesity can lead to Type 2 diabetes (T2D) and obesity is often treated by bariatric surgical procedures; these in turn can lead to excessive GLP-1 secretion resulting in HI.

Germline mutations of at least nine genes causing over-secretion of insulin from pancreatic beta cells have been

associated with congenital HI.^{17,18} Thus, HI can affect patients who are not diabetic, but suffer from loss-of-function mutations of β -cell K_{ATP} channels that cause the most common and severe form of congenital HI, which can lead to brain damage or death if inadequately treated. The autosomal recessive and dominant mutations in *ABCC8/KCNJ11* are the most common cause of medically unresponsive congenital HI.¹⁹ The *ABCC8* and *KCNJ11* genes encode two subunits of the pancreatic beta cell K_{ATP} channel, sulfonylurea type 1 receptor (SUR1) and Kir6.2 (potassium pore).^{20–22} The K_{ATP} channel functions as a metabolic sensor of the pancreatic β -cell that converts the metabolic status to electrical activity via cAMP.²³ This subsequently triggers protein kinase A activation and, in turn, the phosphorylation of the SUR1 subunit of the K_{ATP} channel in an ADP-dependent mechanism thereby facilitating closure of the K_{ATP} channel, followed by membrane depolarization and initiation of insulin release. When K_{ATP} channels open, β -cells hyperpolarize, and insulin secretion is suppressed.²⁴

The GLP-1 receptor is constitutively active in islets of SUR1^{-/-} mice that lack K_{ATP} channels. However, GLP-1 R antagonism by exendin 9–39 (avexitide) has been reported to correct fasting hypoglycemia in SUR1^{-/-} mice by suppressing insulin secretion.²⁵ Exendin 9–39 is a truncated form of exendin-4 that transforms it into a specific GLP-1 R antagonist.²⁶ It has also previously been reported that exendin 9–39 raises fasting blood glucose in normal WT mice.²⁷ Exendin 9–39 has been proposed as a potential therapeutic agent in HI.^{26,28} Thus, the current working hypothesis is that GLP-1 R antagonism will increase fasting blood glucose levels, prevent protein-induced hypoglycemia, and decrease the cellular glucose requirement to maintain euglycemia in subjects with K_{ATP} -associated HI as a result of suppressed insulin secretion and increased glucagon levels with these effects mediated by changes in cellular cAMP levels. Current treatment options are insufficient, with fewer than one-third of newborns and two-thirds of older children responding to approved medical standard of care therapy, which have known side effects or loss of efficacy over time. Loss-of-function mutations in the K_{ATP} channel disrupt this metabolic control. A therapeutic strategy implementing an antibody as treatment for congenital HI and hypoglycemia is validated by the anti-insulin receptor antibody XOMA 358, also known as RZ358.²⁹ Furthermore, a GLP-1 R antagonist antibody could also offer more favorable PK attributes than the exendin 9–39 peptide evaluated in Phase 1 and 1/2 clinical studies (NCT00835328, and NCT00992901).³⁰

Although several GLP-1 R antibodies have been generated for structural and tissue expression studies,^{31–33} no functional activities for these antibodies have been reported. We aimed to identify functional GLP-1 R antibodies and validate our domain-based synthetic GPCR focused library. Here we present the discovery cascade we undertook to rapidly discover a panel of 13 high-affinity GLP-1 R-targeting antibodies. In the resulting IgG panel, the heavy chain complementarity-determining region 3 (HCDR3), which confers most of the binding activity and specificity, was found to include either a GLP-1 motif, a GLP-2 motif, or an unknown/unique sequence. The majority of the GLP-1 R antibodies discovered here are antagonists to the GLP-1 R function; however, we were able to create an agonistic antibody by fusing GLP-1

peptide to the light chain of a nonfunctional GLP-1 R specific antibody. This GPCR-focused antibody discovery platform can be applied to any GPCR of interest, including both antagonists and agonists. The anti-GLP-1 R antibodies discovered here are highly specific for GLP-1 R and had a desirable long half-life in a rat PK study. They display functional activity *in vitro* in cell signaling assays and *in vivo* in healthy wild-type mice. Thus, given the current limited availability of effective GPCR-targeted antibody therapeutics, this study represents an advance for the field of antibody discovery against difficult targets, as well as GPCR drug discovery.

Results

Design of GPCR-focused antibody library is based on GPCR binding motifs and GPCR antibodies

All known GPCR interactions, which include interactions of GPCRs with ligands, peptides, antibodies, endogenous extracellular loops, and small molecules, were analyzed to map the GPCR binding molecular determinants. Crystal structures of almost 150 peptides, ligands or antibodies bound to ECDs of around 50 GPCRs (<http://www.gpcrdb.org>) were used to identify GPCR binding motifs. Over 1000 GPCR binding motifs were extracted from this analysis. In addition, by analysis of all solved structures of GPCRs (zhanglab.ccmb.med.umich.edu/GPCR-EXP/), we identified over 2000 binding motifs from endogenous extracellular loops of GPCRs. Finally, by analysis of structures of over 100 small molecule ligands bound to GPCR, we identified a reduced amino acid library of 5 amino acids (Tyr, Phe, His, Pro and Gly) that may be able to recapitulate many of the structural contacts of these ligands. A sub-library with this reduced amino acid diversity was placed within a CxxxxxC motif. In total, over 5000 GPCR binding motifs were identified (Figure 1). These binding motifs were placed in one of five different stem regions: CARDLRELECEEW_{Txxxxx}SRGPCVDPRGVAGSFDVW, CARDMYDYDF_{xxxxx}EVVPADDAFDIW, CARDGRGSLPRPK

GGP_{xxxxx}YDSEDSGGAFDIW, CARANQHF_{xxxxx}GYHYGMDVW, and CAKHMSMQ_{xxxxx}RADLVGDADFVW.

These stem regions were selected from structural antibodies with ultra-long HCDR3s. Antibody germlines were specifically chosen to tolerate these ultra-long HCDR3s. Structure and sequence analysis of human antibodies with longer than 21 amino acids revealed a V-gene bias in antibodies with long CDR3s. Finally, the germline IGHV (IGHV1-69 and IGHV3-30), IGKV (IGKV1-39 and IGKV3-15) and IGLV (IGLV1-51 and IGLV2-14) genes were chosen based on this analysis.

In addition to HCDR3 diversity, limited diversity was also introduced in the other 5 CDRs. There were 416 HCDR1 and 258 HCDR2 variants in the IGHV1-69 domain; 535 HCDR1 and 416 HCDR2 variants in the IGHV3-30 domain; 490 LCDR1, 420 LCDR2, and 824 LCDR3 variants in the IGKV1-39 domain; 490 LCDR1, 265 LCDR2, and 907 LCDR3 variants in the IGKV3-15 domain; 184 LCDR1, 151 LCDR2, and 824 LCDR3 variants in the IGLV1-51 domain; 967 LCDR1, 535 LCDR2, and 922 LCDR3 variants in the IGLV2-14 domain (Figure 2). These CDR variants were selected by comparing the germline CDRs with the near-germline space of single, double, and triple mutations observed in the CDRs within the V-gene repertoire of at least two of 12 human donors. All CDRs were pre-screened to remove manufacturing liabilities, cryptic splice sites or nucleotide restriction sites. The CDRs were synthesized as an oligo pool and incorporated into the selected antibody scaffolds. The heavy chain variable region (VH) and light chain variable region (VL) genes were linked by (G₄S)₃ linker. The resulting single-chain variable fragment (scFv; VH-linker-VL) gene pool was cloned into a phagemid display vector at the N-terminal of the M13 gene-3 minor coat protein. The final size of our GPCR library is 1×10^{10} in a scFv format. Next-generation sequencing (NGS) was performed on the final phage library to analyze the HCDR3 length distribution in the library for comparison with the HCDR3 length distribution in B-cell populations from three healthy adult donors. The HCDR3 sequences from the three healthy donors used were derived from a publicly available database with over 37 million B-cell receptor sequences.³⁴ The HCDR3 length in our

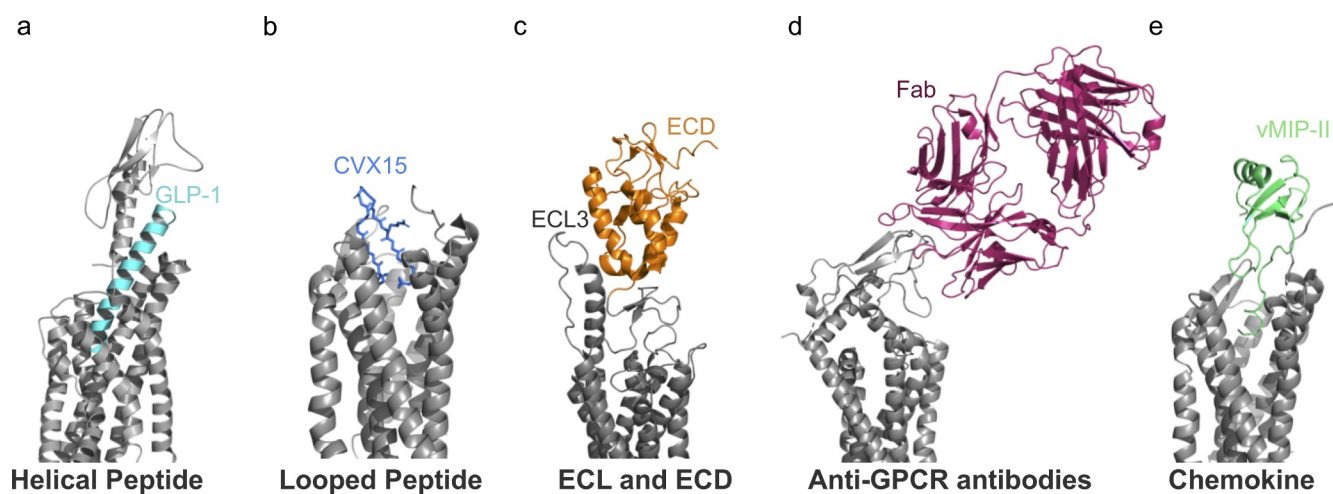


Figure 1. Overview of the subset of available crystal structures of GPCR interactions GPCR-focused library design (a) structure of glucagon-like peptide 1 (GLP-1, cyan) in complex with GLP-1 receptor (GLP-1 R, gray), PDB entry 5VAI. (b) crystal structure of CXCR4 chemokine receptor (gray) in complex with a cyclic peptide antagonist CVX15 (blue), PDB entry 3OR0. (c) crystal structure of the human smoothed with transmembrane domain in gray and extracellular domain (ECD) in orange, PDB entry 5L7D. the ECD contacts the TMD through extracellular loop 3 (ECL3). (d) structure of GLP-1 R (gray) in complex with a GLP-1 R fab7F38 (magenta), PDB entry 6LN2. (e) crystal structure of CXCR4 (gray) in complex with a viral chemokine antagonist viral macrophage inflammatory protein 2 (vMIP-II, green), PDB entry 4RW5.

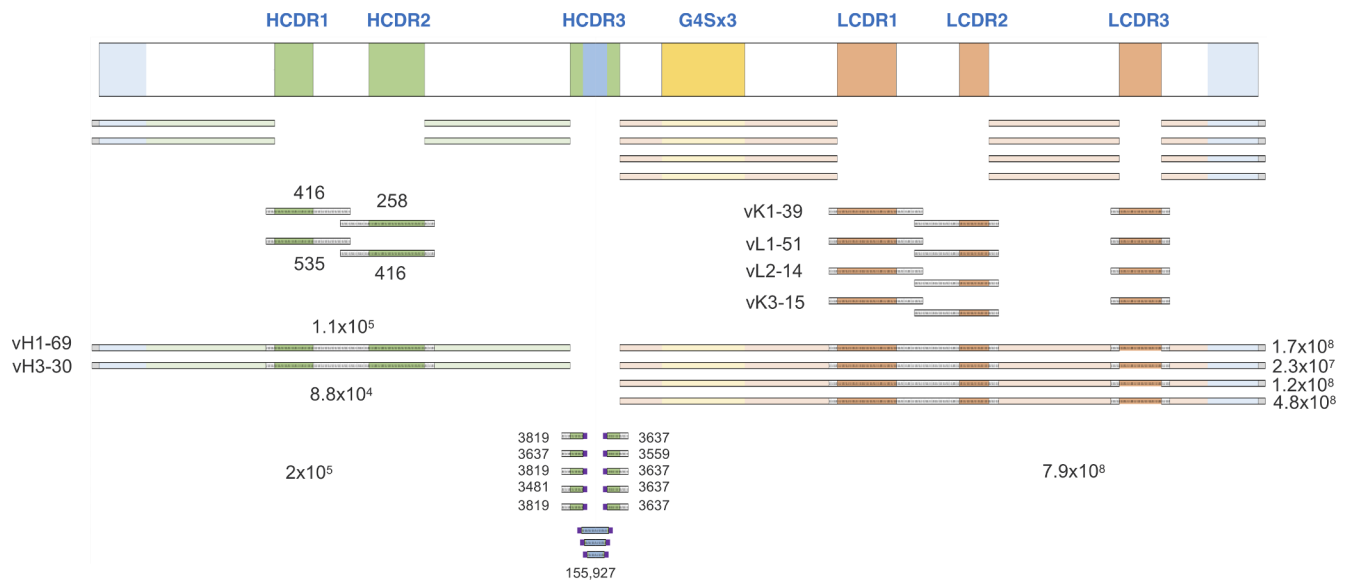


Figure 2. GPCR-focused library design. two germline heavy chain VH1-69 and VH3-30; 4 germline light chain IGKV1-39 and IGKV3-15, and IGLV1-51 and IGLV2-14 were selected as the variable region frameworks. there were 416 HCDR1 and 258 HCDR2 variants in the IGHV1-69 domain; 535 HCDR1 and 416 HCDR2 variants in the IGHV3-30 domain. 155,927 GPCR binding motifs were inserted into the 5 pairs of stem regions: numbered 3819 x 3637; 3637 x 3559; 3819 x 3637; 3481 x 3637; 3819 x 3637. the heavy chain (VH) and light chain (VL) genes were linked by a (G4S)x3 linker.

GPCR library is much longer than the HCDR3 length observed in B-cell repertoire sequences. On average, the median HCDR3 length in our GPCR library (which shows a biphasic pattern of distribution) is two or three times longer (33 to 44 amino acids) than the median lengths observed in natural B-cell repertoire sequences (15 to 17 amino acids) (Figure 3). The biphasic length distribution of HCDR3 in our GPCR library is mainly caused by the two groups of stems (8aa, 9aaxxxxx10aa, 12aa) and (14aa, 16aa xxxxx18aa, 14aa) used to present the motifs within HCDR3.

Phage panning against GLP-1 R-over-expressing cell lines resulted in clonal enrichment

A GLP-1 R-over-expressing Chinese hamster ovary (CHO) stable cell line was created with a FLAG tag presented on the

N-terminus of the receptor to detect cell surface expression and an EGFP tag on the C-terminus to track total receptor expression. Flow cytometry analysis of these cells confirmed that the majority of the receptor (> 80%) was expressed at the cell surface (Figure 4a). These GLP-1 R-expressing CHO cells were used for five rounds of phage panning against the GPCR-focused library. The selection scheme is outlined in Figure 4b. The VH from the output of each panning round was PCR amplified and sequenced by MiSeq. As the percentage of unique HCDR3s decreases in each round output pool, significant clonal enrichment was concurrently observed from round 1 to round 5 (Figure 5), and this indicates we have a target-specific clonal selection in our panning process. In total, ~1000 clones (from round 4 and round 5) were selected for single clonal NGS sequencing and ~100 unique VH-VL pairs were

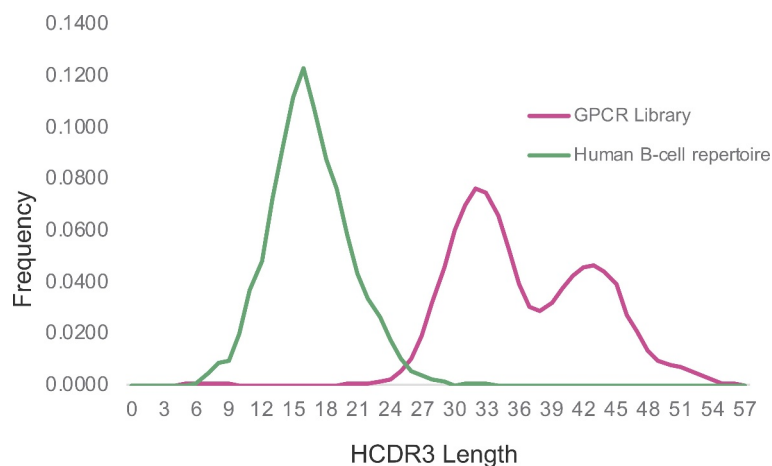


Figure 3. Library GPCR 2.0 HCDR3 length distribution. HCDR3 length distribution in the GPCR-focused library compared to the HCDR3 length distribution in B-cell populations from three healthy adult donors. in total, 2,444,718 unique VH sequences from the GPCR library and 2,481,511 unique VH sequences from human B-cell repertoire were analyzed to generate the length distribution plot.

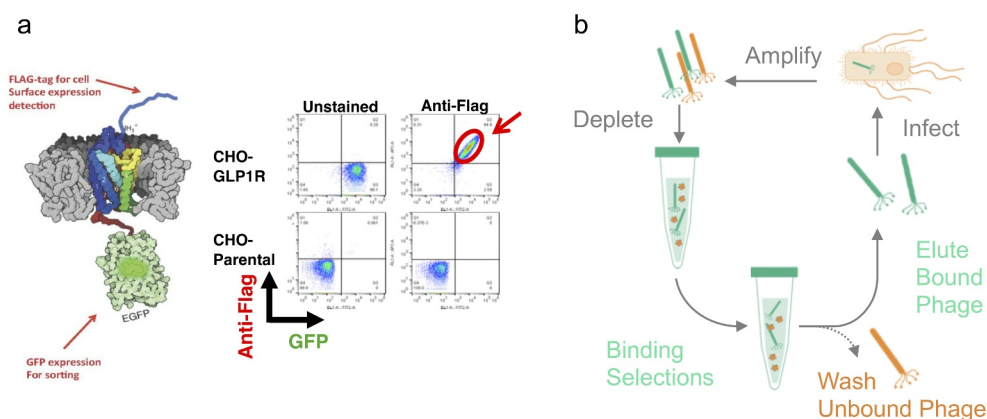


Figure 4. GLP-1 R phage selection scheme (a) the design of over-expressing GLP-1 R CHO cells for the phage antibody library selection. GLP-1 R expression was confirmed by the gating of double detection of GFP green fluorescence and the surface expression of flag tag on the cell surface. (b) cell-based panning process.

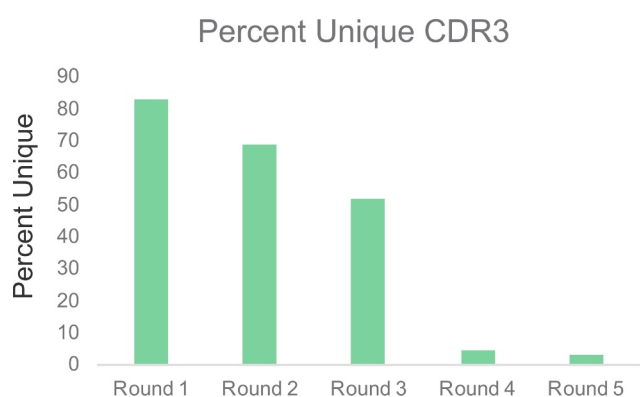


Figure 5. Percentage of unique HCDR3 in the output pools of five GLP-1 R panning rounds. output phage pools from each round of panning were subject to NGS MiSeq 2 x 300bp sequencing. the unique HCDR3s as a percentage of total sequence reads, about 150,000 for each pool. HCDR3 sequences significantly converged after 4 rounds of selection against GLP-1 R-expressing CHO cells.

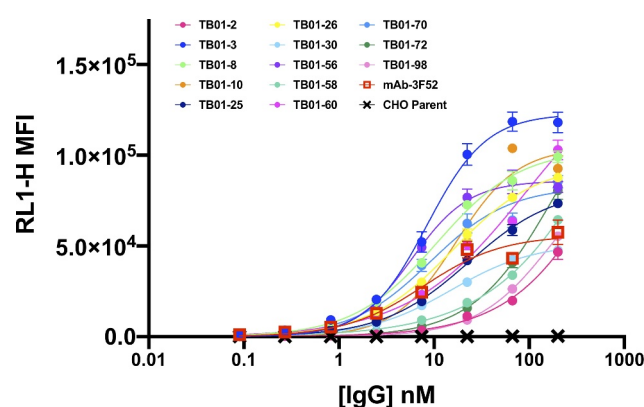


Figure 6. Binding plots of the 13 unique GLP-1 R hits, compared to the parental CHO cell binding. 13 GLP-1 R antibodies identified by single point screening were titrated down from 200 nM concentration with 8-point serial 3-fold dilution. control antibody mAb-3F52 was included to compare its binding affinity to the 13 identified GLP-1 R antibodies. the experiment was done in triplicates with standard error of the mean (SEM) as error bars using graphPad prism 8.

chosen for reformatting and expression as full-length human IgG2 at a 1 ml scale.

IgG binders directed to GLP-1 R contain either GLP-1, GLP-2, or unique HCDR3 motifs identified

Purified IgG clones (**Figure S1 and S2**) expressed by Expi293 cells were tested for specific binding to GLP-1 R-expressing CHO cells. A single-point flow cytometry analysis using 100 nM of IgG concentration revealed that, of 100 IgG unique clones tested, 13 IgG clones bound specifically to GLP-1 R-positive cells (GFP+) and not parental CHO cells (GFP-). The binding of these 13 hits was then further evaluated by 8-point titrations of each IgG clone starting from 200 nM (30 µg/mL) and the cell-binding affinities were determined to be in the double-digit nM range. The average CHO parental cell background binding by all 13 IgG clones is shown as a black line and is minimal compared with specific binding to GLP-1 R-expressing cells (**Figure 6**). We did not see full saturation (the plateau of the binding curve) at the highest concentration, 200 nM, used in the experiment. **Table 1** shows the HCDR3 amino acid sequences of these 13 IgG clones. Six of these were found to include a GLP-1 motif, four included a GLP-2 motif, and three had an unknown motif.

Eight IgGs of the 13 binders are antagonists in GLP-1 R mediated cAMP signaling

The 13 IgG binders were next assessed for their functional activity in the cAMP signaling pathway by using GLP-1 R-over-expressing CHO-K1 cells purchased from DiscoverX that are designed and validated for assessing GLP-1 R-induced cAMP signaling. In the first instance, the IgG clones were tested for agonist activity as compared with the peptide agonist GLP-1 7–36 in dose titrations. While GLP-1 7–36 stimulation resulted in a cAMP signal, none was observed for the IgG clones, indicating that they are not activating. Subsequently, the panel of IgG clones was tested for antagonist activity by pre-incubating GLP-1 R-expressing cells with a threefold titration down from 100 nM IgGs to allow binding to occur and then stimulating the cells with the agonistic GLP-1 7–36 or Exendin-4 at EC50 concentration. This allowed examination of the effect of IgGs and control antagonist Exendin 9–39 titration on GLP-1 7–36 and Exendin-4 -induced GLP-1 R cAMP signaling, thereby evaluating any potential competitive effects of the IgGs. It was observed that 8 of the 13 IgG clones can compete the agonistic peptide's cAMP activity in a dose response manner, suggesting that they act as competitive antagonists of the GLP-1 7–36 response (**Figure 7a**). Similar observations were made regarding the effect of the 8 IgG clones on Exendin-4-induced GLP-

Table 1. HCDR3 loop sequences of the 13 unique GLP-1 R binders. six of the clones have a GLP-1 motif, four of the clones have a GLP-2 motif, and three clones do not have a GLP-1 or GLP-2 motif. for the clones that have the GLP-1 or GLP-2 motif, residues that are similar to the GLP-1 sequence or the GLP-2 sequence are colored in blue or green respectively, and the residues that are different are colored red. functional antagonists in the cAMP assay are highlighted in yellow.

	HCDR3
GLP-1	HAEGTFTSDVSSYLEGQAAKEFIAWLVKGRG
TB01-3	HMSMQEGAVTGEQAAKEFIAWLVKGRVRADLVGDAFDV
TB01-8	DGRGSLPRPKGGPQTVGEQAAKEFIAWLVKGLTYDSSSEDSGGAFDI
TB01-56	ANQHFFSGAEGEGQAAKEFIAWLVKGIIPGYHYGYMDV
TB01-58	ANQHFGLHAQEGEGQAAKEFIAWLVKSGTYGYHYGYMDV
TB01-60	HMSMQDYLVIGEGQAAKEFIAWLVKGGPARADLVGDAFDV
TB01-72	DMYYDFHPEGTFTSDVSSYLEGQAAKEFIAWLVKGLIYEVVPADDAFDI
GLP-2	HADGSFSDEMNTILDNLAARDFINWLIQTKITD
TB01-25	ANQHFLSHAGAARDFINWLIQTKITGLGSGYHYGYMDV
TB01-30	DMYYDFLKGIDNLAARDFINWLIQTKITDGTDEVPADDAFDI
TB01-70	DGRGSLPRPKGGPPSSGRDFINWLIQTKITDGFYDSSSEDSGGAFDI
TB01-98	DMYYDFGYFTGMNTILDNLAARDFINWLIQTKITDRGGSGSGSGSGSGSGSEVPADDAFDI
TB01-2	DMYYDFETVVEGIQWYEALKAGKLGEVVPADDAFDI
TB01-10	ANQHFFVPGSLKVWLKGVAPESSEYDSSSEDSGGAFDI
TB01-26	HMSMQEGVLQGQIPSTIDWEGLLHLIRADLVGDAFDV

1 R cAMP signaling response (Figure 7b). The remaining five IgG clones appeared to have no significant effects on GLP-1 R cAMP signaling (data not shown).

Characterization of mechanisms of action of the antagonist IgG TB01-3

To determine the mechanism of action of these resulting functional hits, we focused on one of the GLP-1 motif-containing IgG clones that demonstrated high binding affinity, as well as functionality: TB01-3. Ligand competition binding assays, the IgG effects on the GLP-1 dose response in cAMP signaling, and beta-arrestin recruitment assays were conducted, resulting in the following characterization of TB01-3.

Competition with the endogenous ligand in GLP-1 R binding assays

To determine if TB01-3 binds to the orthosteric site on the receptor, N-terminal FLAG-tagged and C terminal GFP-tagged GLP-1 R-over-expressing CHO cells were incubated with a dose titration of TB01-3 starting at 100 nM in the presence or absence of a fixed concentration of the peptide agonist GLP-1 7-36 (1 μ M). Flow cytometry analysis revealed significantly reduced binding of TB01-3 to GLP-1 R (GFP+) in the presence of GLP-1 7-36. Whilst the presence of GLP-1 7-36 peptide does not completely ablate TB01-3 binding, this observation suggests that the antibody may bind to an overlapping epitope, or GLP-1 7-36 confers a conformational change on the receptor reducing the binding affinity of TB01-3 for GLP-1 R. (Figure 8a).

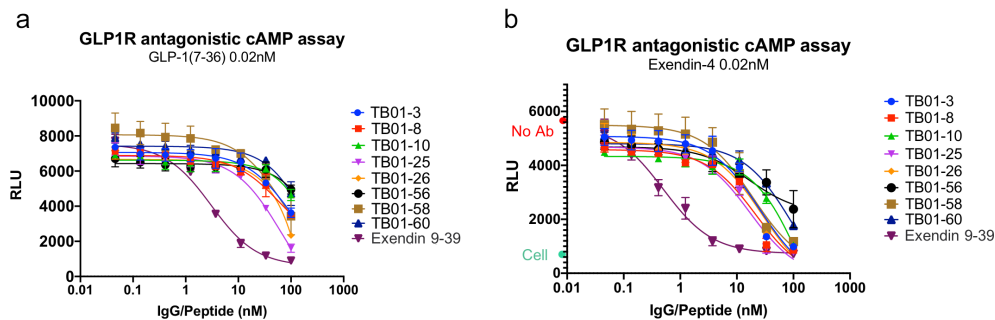


Figure 7. Antagonistic cAMP assay of GLP-1 R antibodies (a) the titrated 8 GLP-1 R antibodies and antagonist control exendin 9-39 were tested for antagonistic effects with a fixed concentration of 0.02 nM GLP-1(7-36) activity in a cAMP assay. (b) the titrated 8 GLP-1 R antibodies and antagonist control xendin 9-39 were tested for antagonistic effects with a fixed concentration of 0.02 nM exendin-4 activity in a cAMP assay. experiments were performed in duplicates and the error bars were represented as the standard error of the mean, SEM.

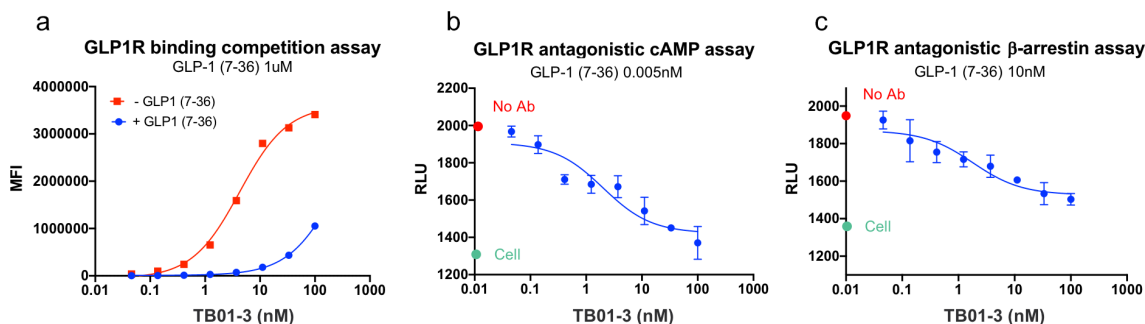


Figure 8. TB01-3 competes with GLP-1(7-36) peptide for binding and activities (a) inhibition of TB01-3 binding in the absence and presence of GLP-1(7-36). (b) TB01-3 is a competitive antagonist of the GLP-1 activation in the cAMP assay (c) TB01-3 is also an antagonist in the GLP-1 induced β -arrestin recruitment. experiments were conducted in duplicates, and the standard error of the mean, SEM were plotted as error bars for Figure B and C.

TB01-3 antagonizes GLP-1 activated cAMP signaling

The next step was to determine if TB01-3 exhibits antagonism for GLP-1 R in a dose-dependent manner. When GLP-1 7-36-induced cAMP

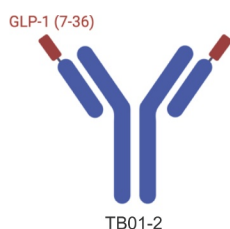


Figure 9. Design of TB59-2. the GLP1 (7-36) peptide was linked to the N-terminal of light chain of the functionally inactive GLP-1 R binding antibody TB01-2 with a (G4S)x3 linker.

signaling was examined in the presence of a constant concentration (0.005 nM) of GLP-1 7-36 with a dose titration of TB01-3 starting at 100 nM and a 3-fold down titration, a clear dose-dependent inhibition of the cAMP signal was observed. TB01-3 can completely inhibit GLP-1 7-36 activity, with an IC_{50} around 5 nM (Figure 8b), suggesting that TB01-3 is a competitive antagonist to the GLP-1 7-36 peptide.

TB01-3 reduces β -arrestin recruitment upon GLP-1 R activation

When a GPCR is activated by an agonist, β -arrestins are recruited to the GPCR from the cytosol, thereby excluding

the receptor from further G protein interactions and leading to signal arrest, hence the name “arrestin”.³⁵ To determine if TB01-3 had any effects on β -arrestin recruitment by activated GLP-1 R, GLP-1 R-over-expressing CHO-K1 cells (DiscoverX) that are specifically designed and validated for assessing GLP-1 R β -arrestin recruitment were used in the following manner. Cells were pre-incubated with a 3-fold titration of TB01-3 from 100 nM down for 1 hr at room temperature (RT) to allow binding to occur and then stimulated with 10 nM GLP-1 7-36. TB01-3 demonstrated inhibition of GLP-1 7-36 peptide-induced beta arrestin recruitment to GLP-1 R in a dose-response curve for β -arrestin recruitment (Figure 8c). This indicated that TB01-3 reduces β -arrestin recruitment to GLP-1 R, which is consistent with the observed reduced receptor activation. Thus, these cell-based assays indicate that TB01-3 is an antagonist to GLP-1 7-36 for GLP-1 R.

Design and characterization of a GLP-1 R agonist IgG TB59-2

Since none of the 13 IgG hits showed any agonist activity, we engineered a GLP-1 R agonist antibody (TB59-2) by linking the native GLP-1 7-36 peptide with a (G4S)x3 linker to the light chain N-terminal of a functionally inactive but GLP-1 R-specific binder, TB01-2 (Figure 9). GLP-1 R binding assays, cAMP assays, and β -arrestin recruitment assays were conducted, resulting in characterization of TB59-2 as described below.

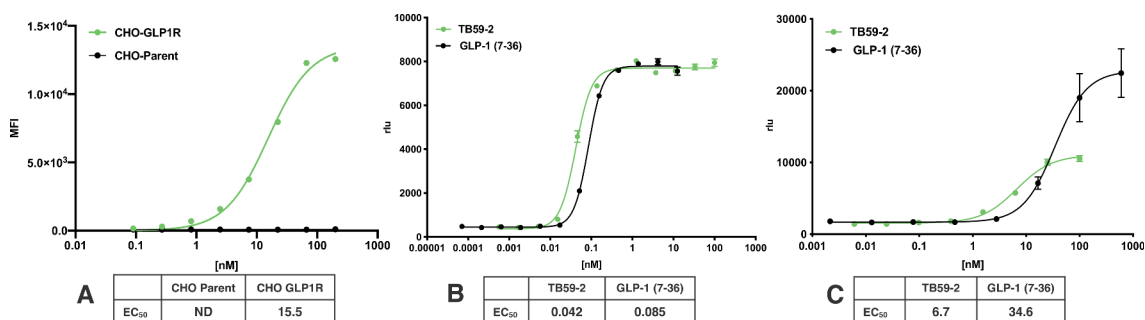


Figure 10. TB59-2 is a potent agonist of the GLP-1 R (a) TB59-2 binds specifically to the GLP-1 R with an EC_{50} of 15.5 nM. (b) TB59-2 is a potent agonist in the cAMP assay with a similar EC_{50} as the GLP-1 7-36 peptide. (c) TB59-2 can also induce the β -arrestin recruitment in GLP-1 R expression cells. experiments were conducted in duplicates, and the standard error of the mean, SEM were plotted as error bars for Figure B and C.

TB59-2 specifically binds to GLP-1 R-expressing CHO cells

Flow cytometry analysis revealed that TB59-2 bound specifically to GLP-1 R-positive cells (GFP+) and not parental CHO cells (GFP-), specific binding was also confirmed by TB59-2 dose titrations, producing an apparent binding EC_{50} of 15.5 nM (Figure 10a).

TB59-2 induces a GLP-1 R cAMP response similar to GLP-1 7-36

TB59-2 was tested for agonist activity as compared with GLP-1 7-36 for stimulating GLP-1 R-over-expressing CHO-K1 cells (DiscoverX), with separate dose titration analyses conducted for both ligand and

antibody. Both induced similar cAMP signaling profiles and their dose-response curves had almost overlapping EC_{50} values, 0.042 nM for TB59-2 and 0.085 nM for GLP-1 7-36 (Figure 10b), supporting the hypothesis that TB59-2 can act as an effective agonist for GLP-1 R.

TB59-2 is less efficacious for β -arrestin recruitment to GLP-1 R than GLP-1 7-36

To determine if TB59-2 was able to induce a similar level of β -arrestin recruitment upon GLP-1 R activation as GLP-1 7-36, GLP-1 R-over-expressing CHO-K1 cells (DiscoverX) were stimulated with dose titrations of each. We found that less β -arrestin recruitment occurred with TB59-2 stimulation than with GLP-1 7-36 stimulation (Figure 10c). TB59-2 can induce β -arrestin recruitment as the agonist GLP-1

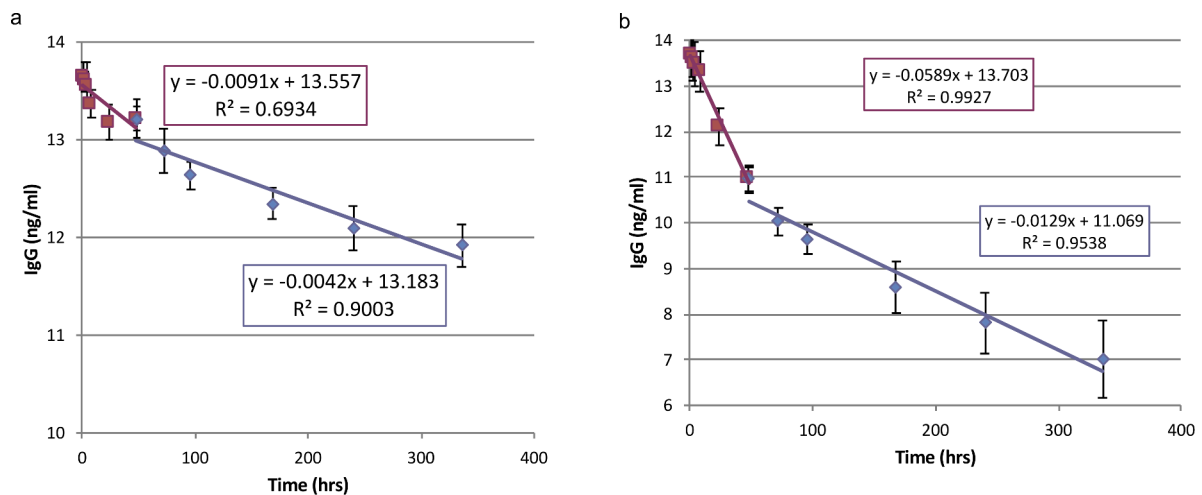


Figure 11. The in vivo PK and PD study of both the antagonistic and agonistic antibodies, TB01-3 and TB59-2 (a) TB01-3 has a fast-alpha phase and an equilibrium beta phase. based on the beta phase calculation, TB01-3 has a 1-week half-life in rat. (b) TB59-2 has a 2-day half-life in rat. there are 5 rats used in each group, the error bars are plotted as the SD.

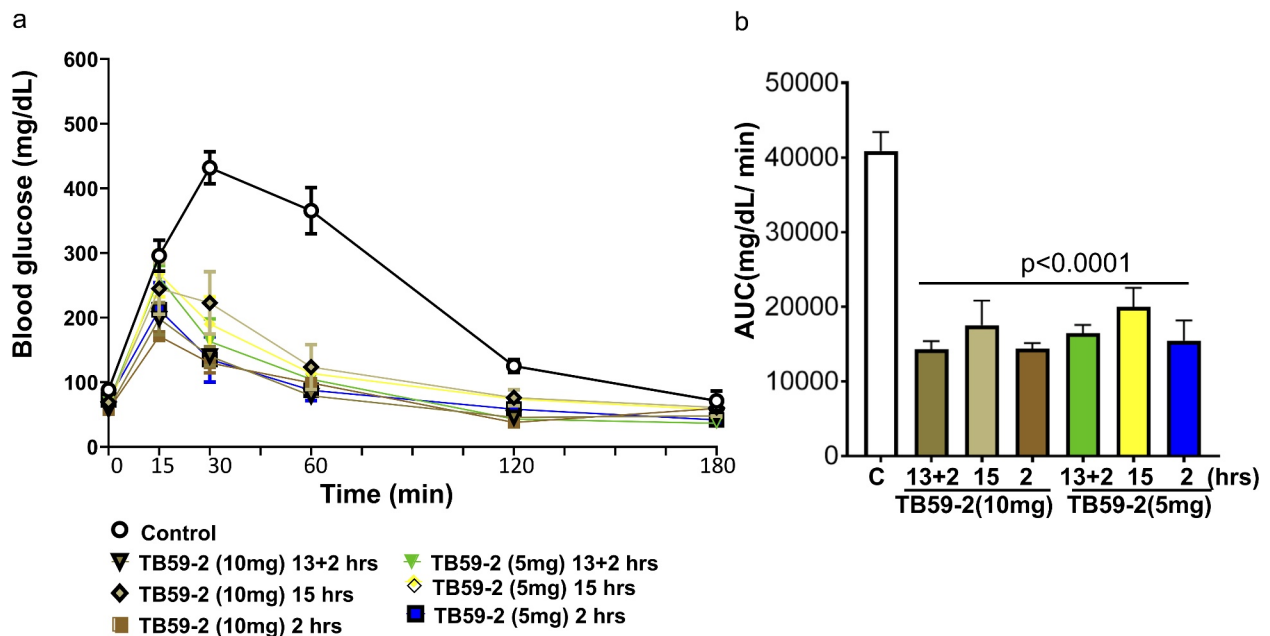


Figure 12. TB59-2 functions as an agonist in lowering the blood glucose level in a glucose tolerance test (a) agonist mAb treatment, either dose or dosing regimen, significantly stabilizes blood glucose even after a glucose challenge. (b) compared to control mice agonist mAb treatments are all significant ($p < .001$) at reducing area under the curve (AUC) in an GTT. however, there is no significant difference between each individual treatment timing or dose. the GTT AUC was analyzed by ordinary one-way Anova with graphpad prism 8. the error bars are plotted as SD with 5 mice in each group.

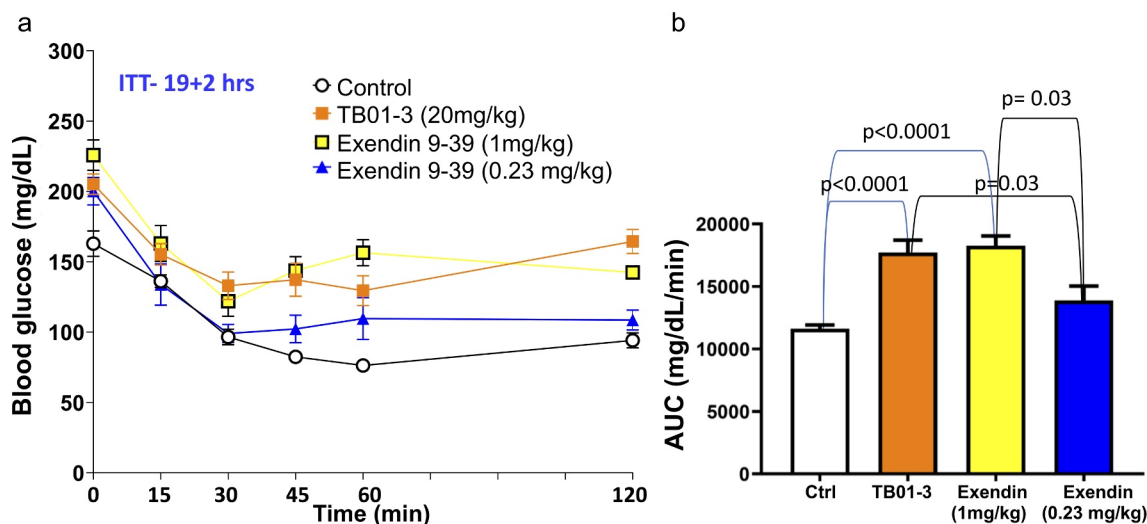


Figure 13. Antagonists TB01-3 and exendin 9–39 stabilize a higher blood glucose level in a mouse insulin tolerance test (a) antagonist, TB01-3 mAb and GLP-1 peptide exendin 9–39 treatment, 19 + 2 hour dosing regimen, significantly stabilizes a higher blood glucose after an insulin challenge. TB01-3 vs control has a p value < .05 and TB01-3 vs exendin (0.23 mg) has $p = .0009$, both are significant. (b) compared to control mice TB01-3 mAb (20 mg/kg) and exendin (1 mg/kg) treatments, 19 + 2 hours, are both significant ($p < .0001$) at stabilizing area under the curve (AUC) in an ITT. However, there is no significant difference between TB01-3 and control vs. exendin (0.23 mg/kg) 19 + 2 hour treatment. The AUC in B was analyzed by ordinary one-way anova, and the p value in Figure A was analyzed by unpaired t test.

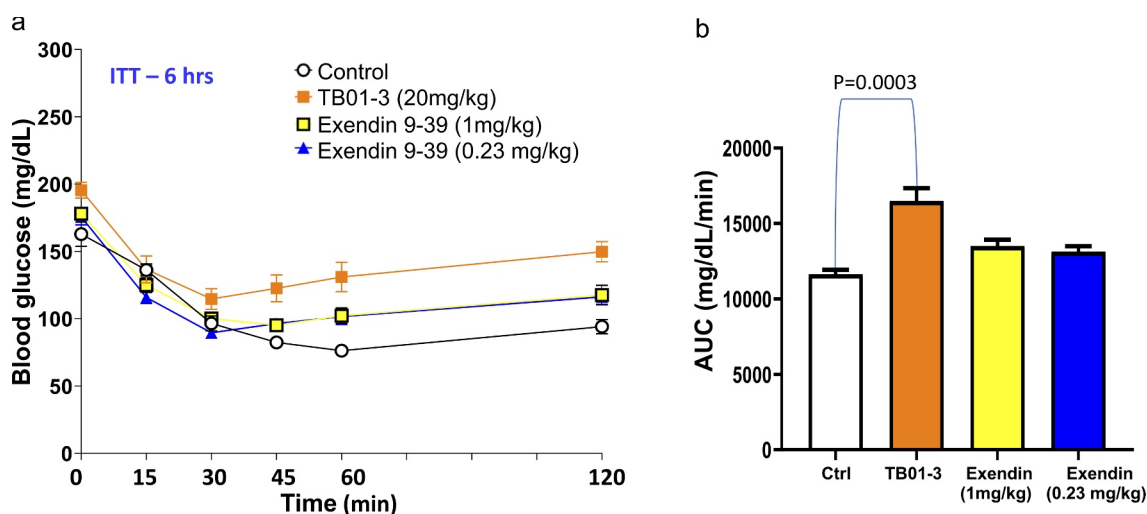


Figure 14. TB01-3 and exendin 9–39 treatment in a single 6-hour dosing insulin tolerance test. (a) antagonist, TB01-3 mAb treatment significantly stabilizes a higher blood glucose after an insulin challenge compared to GLP-1 peptide exendin 9–39 (1.0 or 0.23 mg/kg dose) or control. Both TB01-3 vs control and TB01-3 vs exendin (1.0 mg or 0.23 mg dose) have a $p < .05$, both are significant. (b) compared to control mice, TB01-3 mAb (20 mg/kg) treatment at 6 hours, significantly ($p = .0003$) stabilizes area under the curve (AUC) in an ITT. The ITT AUC in Figure B was analyzed by ordinary one-way anova, and the p value in Figure A was analyzed by unpaired t test.

peptide, 7–36 does, but it is less efficacious than GLP-1 7–36 to induce maximal β -arrestin recruitment.

In vivo PK and PD testing of TB01-3 and TB59-2

Endogenous GLP-1 peptide has a very short serum half-life of only a few minutes, but GLP-1 R antibodies can have significantly longer half-lives. This can be a considerable advantage over the current GLP-1 peptide analog therapeutics. We performed an *in vivo* PK rat study to evaluate the half-life of the antagonist TB01-3 and agonist TB59-2 in IgG format. In a 2-week PK study, TB01-3 exhibited an antibody-like *in vivo* half-life of ~1-week in rats, while the

agonist GLP-1 peptide-antibody fusion, TB59-2 exhibited >2-day half-life in rats (Figure 11a and Figure 11b). Liraglutide, the approved GLP-1 R agonist for the treatment of T2D has a 13-hour half-life.¹³

Agonist TB59-2 was tested for *in vivo* pharmacodynamic (PD) effects in the glucose tolerance test (GTT) using a wild-type C57BL/6NHsd mouse model, in comparison with the vehicle control. Agonist monoclonal antibody (mAb) TB59-2 treatment, implementing either dose levels (5 mg/kg and 10 mg/kg) or dosing regimen (2 hrs, 13 + 2 hrs, and 15 hrs before glucose challenge), significantly stabilized blood glucose even after a glucose challenge (Figure 12a). Compared to control mice, TB59-2 treatments are all significant ($p < .001$) at reducing Area Under the Curve (AUC) in a GTT (Figure 12b), but there is

no significant difference between each individual treatment timing or dose.

Antagonist, TB01-3 mAb, and GLP-1 peptide Exendin 9–39 treatment, with 19 + 2 hours dosing regimen before insulin challenge, significantly stabilizes a higher blood glucose in wild-type C57BL/6NHSd mice (Figure 13a). Compared to control mice TB01-3 mAb (20 mg/kg) and Exendin (1 mg/kg) treatments are both significant ($p < .0001$) at stabilizing AUC in an Insulin Tolerance test (ITT) (Figure 13b). However, there is no significant difference between TB01-3 and Control vs. Exendin (0.23 mg/kg) with 19 + 2-hour treatment. In another experiment using single 6-hour dosing regimen, antagonist, TB01-3 mAb treatment also significantly stabilized a higher blood glucose after an insulin challenge compared to GLP-1 peptide Exendin 9–39 (1.0 or 0.23 mg/kg dose) or control (Figure 14a). Compared to control mice, TB01-3 mAb (20 mg/kg) treatment at 6 hours significantly ($p < .05$) stabilizes AUC in an ITT. However, there is no significant difference between Control vs. Exendin (1.0 and 0.23 mg/kg) with the single 6-hour treatment (Figure 14b).

Discussion

It is challenging to generate any antibodies against GPCR targets, and more so for functional anti-GPCR antibodies³⁶ due in part to the low levels of GPCR cell expression and accessibility of the epitopes presented on the exposed portion outside the cell surface. The two approved GPCR antibody drugs, mogamulizumab and erenumab, both target the relatively large and stable N-terminal extracellular domain, but may not truly represent the full opportunity for anti-GPCR antibodies.^{37,38} To address this challenge and increase the probability of identifying functional antibodies targeting GPCRs, we designed a synthetic human GPCR-focused antibody library. Modeled on natural GPCR receptor–ligand interactions, the library design takes into consideration all different types and orthologs of GPCR-binding motifs and incorporates over 150,000 of them into the antibody heavy chain CDR3. By using Twist Precision DNA synthesis technology, we created a high quality 1×10^{10} diversity library with 100% pre-designed antibody sequences. The library lacks all pre-specified manufacturability liabilities, such as unpaired cysteines, isomerization, cleavage, deamidation, and glycosylation sites, and was constructed with the most commonly used human heavy and light chain frameworks.

To generate proof of concept data for this GPCR-focused library, we identified a panel of 13 unique and specific GLP-1 R binding antibodies after 5 rounds of cell panning. The panning selection greatly enriched antibodies that contain the GLP-1 peptide motifs in 6 of the 13 GLP-1 R binders. We even found 4 antibodies that have the GLP-2 peptide motifs in the HCDR3 region. To our knowledge, it has not been reported that the GLP-2 peptide binds GLP-1 R. We tested our 13 lead antibodies, including the 4 with GLP-2 peptide motifs, and confirmed that they do not bind to GLP-2 R-expressing cells, and have no activity in a GLP-2 R cAMP assay (data not shown). Potentially, the GLP-2 motif in HCDR3 may have weak GLP-1 R binding affinity and combined together with HCDR1 and HCDR2, as well as the light chain, most likely assisted to increase binding affinity to GLP-1 R, thereby inducing antagonist function in the cAMP assay. Interestingly, we also found 3 antibodies that bind strongly to GLP-1 R with no identifiable motif in the HCDR3. This result indicates that sufficient diversity exists in our library beyond the main incorporated motifs derived from GPCR antibodies and small ligand mimetics. The

majority of binders containing the GLP-1 motif are also antagonists, with only one clone that contains the GLP-2 motif as a functional inhibitor (Table 1). This indicates that other components of antibody structure, such as the HCDR1 and HCDR2, as well as the light chain, can also influence antibody binding and function. Besides testing on GLP-1 R and GLP-2 R for binding and function, we did not test binding of our antibodies to other related receptors, like the GIP and glucagon receptors.

We did not identify an agonist from 5 rounds of selection with the GPCR-focused library. To create a GLP-1 R agonistic antibody, we used the nonfunctional TB01-2, which does not have a GLP-1 or GLP-2 peptide motif in the parental antibody, and fused wild-type GLP-1 peptide 7–36 to the N-terminal of the light chain. The resulting peptide-antibody fusion, TB59-2, has a comparable binding affinity as the GLP-1 free peptide to GLP-1 R-expressing CHO cells, and also has comparable function in the agonistic format of the cAMP activity assay. The great advantage for TB59-2 is the length of *in vivo* half-life compared to the GLP-1 peptide agonist. We tested the agonistic TB59-2 for *in vivo* PK in normal rats. TB59-2 has a 2-day half-life in our rat model studies using 10 mg/kg dosing and based on the measurement of the full GLP-1 peptide presence in the blood samples. This is significantly longer than the extremely short half-life of the GLP-1 peptide, and could mean a potentially much longer dosing interval as required for diabetic patients, particularly when administered as an injectable therapeutic. TB59-2 is fully functional in lowering blood glucose level in wild-type mice after a glucose challenge and is effective in controlling glucose even 15 hours after dosing at 5 mg/kg. This is consistent with the half-life assessment of 2 days in rat. A recent study on Everestmab also used a similar approach to generate a GLP-1 R agonist by fusion of the GLP-1 peptide to an anti-GLP-1 R nanobody.³⁹

Both the agonists and antagonists of GLP-1 R have therapeutic applications. The longer half-life GLP-1 peptide analogs, such as liraglutide (Victoza), dulaglutide (Trulicity), and semaglutide (Ozempic) are widely used in treating T2D patients. TB59-2 demonstrates that we can create an agonist with a longer half-life by fusing the GLP-1 peptide ligand to a nonfunctional specific GLP-1 R binder. Having an *in vivo* half-life similar to the dulaglutide's 2-day half-life,¹³ TB59-2 has the potential to achieve once-weekly dosing in treating the T2D patients. Besides use of albumin (albiglutide), Fc (dulaglutide) and antibody GLP-1 peptide fusion to increase the half-life, a recent report demonstrated that conjugation of agonistic peptide to an inert antibody through free cysteine in HCDR3 can also achieve improved half-life and *in vivo* activities.⁴⁰ All these approaches broaden the opportunities for generating functional protein therapeutics through antibody engineering.

GLP-1 R antagonists can also have important applications in preventing hypoglycemia incidents for congenital HI, diabetes, and post-bariatric HI, with proof of concept provided by studies using exendin 9–39 (Ex-9 or avexitide) (a truncated form of the GLP-1 agonist exendin-4 and a specific GLP-1 receptor antagonist²⁵), in glucose homeostasis in subjects with congenital HI. However, with a half-life 3.5 to 4 hr,⁴¹ avexitide has to be administered by continuous intravenous infusion, but has demonstrated complete reversal of HI. Our GLP-1 R antagonistic antibody TB01-3 showed a comparable effect in raising blood glucose levels after an insulin challenge to the 1 mg/kg dosing of Ex-9, but only with the 19 + 2 hours dosing. For the 6 hours dosing ITT experiment, the TB01-3

demonstrated a much better blood glucose-raising function that is statistically significant than the Ex-9, which had no significant difference with buffer control, and this is consistent with the avexitide's ~4 hr half-life. On the other hand, TB01-3 has a half-life of 1 week in rat and is anticipated to show a much longer half-life in human, thereby offering a potential advantage over avexitide in treating HI. This could be confirmed by further study in cynomolgus monkeys. Given the lack of available therapies, antagonism of the GLP-1 receptor to control hypoglycemia by TB01-3 could have a beneficial effect on patient compliance and improve long-term outcomes for the devastating congenital HI disorder.

As demonstrated by previously reported observations involving the insertion of the CXCR4-binding cyclic peptide CVX15⁴² and Exendin-4⁴³ into the bovine antibody (BLV1H12) HCDR3, we have expanded the principle further to encompass all known endogenous GPCR binding motifs in our GPCR-focused library. With the greater than a million combinations derived from the 5 other CDRs and frameworks, this engineered strategy will likely provide a cooperative environment for the introduced binding motif in the HCDR3 to function in a directed evolution process. The successful identification of GLP-1 R antibodies presented here provides the first proof of concept data, demonstrating both *in vitro* and *in vivo* functionality, behind our GPCR-focused library design. Our goal is to expand the work to show the library can be applied to many other GPCR targets and our platform can be used to rapidly generate therapeutic human GPCR antibodies.

Materials and methods

All research reported here was conducted in an ethical and responsible manner and is in full compliance with all relevant codes of experimentation and legislation. All work was conducted with the formal approval of the local animal care committees: the Charles River Institutional Animal Care and Use Committee (IACUC) and IACUC at the University of California, San Francisco (UCSF).

Stable cell line and phage library generation

The full-length human GLP-1 R gene (UniProt – P43220) with an N-terminal FLAG tag and C-terminal GFP tag cloned into pCDNA3.1(+) vector (ThermoFisher) was transfected into suspension CHO cells to generate the stable cell line expressing GLP-1 R. Target expression was confirmed by fluorescence-activated cell sorting. Cells expressing >80% of GLP-1 R by GFP were then directly used for cell-based selections.

Germline heavy chain IGHV1-69, IGHV3-30 and germline light chain IGKV1-39, IGKV3-15, IGLV1-51, IGLV2-14 framework combinations were used in the GPCR-focused phage-displayed library, and all six CDR diversities were encoded by oligo pools synthesized by Twist Bioscience. The CDRs were also screened to ensure they did not contain manufacturing liabilities, cryptic splice sites, or commonly used nucleotide restriction sites. The VH and VL were linked by (G4S)₃ linker. The resulting scFv (VH-linker-VL) gene library was cloned into a pADL 22–2 c

(Antibody Design Labs) phage display vector by NotI restriction digestion and electroporated into TG1 electro-competent *E. coli* cells. (Lucigen). The final library has a diversity of 1.1×10^{10} size, which was verified by NGS to ensure good representation of our design.

Panning and screening strategy used to isolate agonist GLP-1 R scFv clones

Before panning on GLP-1 R-expressing CHO cells, phage particles were blocked with 5% bovine serum albumin (BSA)/phosphate-buffered saline (PBS) and depleted for nonspecific binders on CHO parent cells. For CHO parent cell depletion, the input phage aliquot was rotated at 14 rpm/min with 1×10^8 CHO parent cells for 1 hour at RT. The cells were then pelleted by centrifuging at 1,200 rpm for 10 mins in a tabletop Eppendorf centrifuge 5920RS/4x1000 rotor to deplete the non-specific CHO cell binders. The phage supernatant, depleted of CHO cell binders, was then combined with 1×10^8 GLP-1 R-expressing CHO cells. The phage supernatant and GLP-1 R-expressing CHO cells were rotated at 14 rpm/min for 1 hour at RT to select for GLP-1 R binders. After incubation, the cells were washed several times with 1x PBS/0.5% Tween to remove non-binding clones. To elute the phage bound to the GLP-1 R-expressing cells, the cells were incubated with trypsin in PBS buffer for 30 minutes at 37°C. The cells were pelleted by centrifuging at 1,200 rpm for 10 mins. The output supernatant enriched in GLP-1 R binding clones was amplified in TG1 *E. coli* cells to use as input phage for the next round of selection. This selection strategy was repeated for five rounds. Every round was depleted against the CHO parent background. Amplified output phage from a round was used as the input phage for the subsequent round, and the stringency of washes were increased in each subsequent round of selections with more washes. After five rounds of selection, 500 clones from each of round 4 and round 5 were Sanger sequenced to identify unique clones.

Next-generation sequencing analysis

The phagemid DNA was miniprep from the output bacterial stocks of all panning rounds. The VH was PCR amplified from the phagemid DNA using the Forward Primer ACAGAATTCATTAAGAGAGAAATTAACC and reverse primer TGAACCGCCTCCACCGCTAG. The PCR product was directly used for library preparation using the KAPA HyperPlus Library Preparation Kit (Kapa Biosystems, product # KK8514). To add diversity in the library, the samples were spiked with 15% PhiX Control purchased from Illumina, Inc. (product # FC-110-3001). The library was then loaded onto Illumina's 600 cycle MiSeq Reagent Kit v3 (Illumina, product # MS-102-3003) and run on the MiSeq instrument.

Reformatting and High Throughput (HT) IgG purification

Expi293 cells were transfected using Expifectamine (ThermoFisher, A14524) with the heavy chain and light chain DNA at a 2:1 ratio and supernatants were harvested 4 days post-transfection before cell viability dropped below 80%. Purifications were undertaken using either King Fisher (ThermoFisher) with protein A magnetic beads or

Phynexus protein A column tips (Hamilton). An Akta HPLC purification system (GE) was used for large-scale production of IgG clones that were evaluated in *in vivo* mouse studies.

IgG characterization and quality control. The purified IgGs for the positive GLP-1 R binders (hits) were subjected to characterization for their purity by LabChip GXII Touch HT Protein Express high-sensitivity assay. Dithiothreitol (DTT) was used to reduce the IgG into VH and VL. IgG concentrations were measured using Lunatic (UnChain). IgG for *in vivo* mouse studies were further characterized by HPLC and tested for endotoxin levels (Endosafe[®] nexgen-PTS[™] Endotoxin Testing, Charles River), with less than 5 EU per kg dosing.

Binding assays and flow cytometry

GLP-1 R IgG clones were tested in a binding assay coupled to flow cytometry analysis as follows: FLAG-GLP-1 R-GFP-expressing CHO cells (CHO-GLP-1 R) and CHO parent cells were incubated with 100 nM IgG for 1 h on ice, washed three times and incubated with Alexa 647 conjugated goat-anti-human antibody (1:200) (Jackson ImmunoResearch Laboratories, 109-605-044) for 30 min on ice, followed by three washes, centrifuging to pellet the cells between each washing step. All incubations and washes were in buffer containing PBS+1% BSA. For titrations, IgG was serially diluted 1:3 starting from 100 nM down to 0.046 nM. Cells were analyzed by flow cytometry and hits (i.e., an IgG that specifically binds to CHO-GLP-1 R) were identified by measuring the GFP signal against the Alexa 647 signal. Flow cytometry data of binding assays with 100 nM IgG are presented as dot plots. Analyses of binding assays with IgG titrations are presented as binding curves plotting IgG concentrations against mean fluorescence intensity.

Ligand competition assay

Ligand competition assays involved co-incubating the primary IgG with 1 μ M GLP-1 (7–36). For each data point, IgG (600 nM) was prepared in Flow buffer (PBS+1%BSA) and diluted 1:3 down for 8 titration points. Peptide GLP-1 7–36 (2 μ M) was prepared similarly with the Flow buffer (PBS+1% BSA). Each well contained 100,000 cells to which 50 μ L of IgG and 50 μ L of peptide (=plus) or buffer alone without peptide (=minus) were added. Cells and IgG/peptide mix were incubated for 1 hr on ice, and after washing, secondary antibody (goat anti-human APC, Jackson ImmunoResearch Laboratories, product #109-605-044) diluted 1:200 in PBS+1%BSA was added. This was incubated on ice for 30 mins (50 μ L per well), before washing and resuspending in 60 μ L buffer. Finally, the assay read-out was measured on an Intellicyt[®] IQue3 Screener at a rate of 4 seconds per well.

Cell-based functional assays

cAMP assay

GLP-1 R IgG clones were tested for their potential effects on GLP-1 R signaling by performing cAMP assays obtained from Eurofins DiscoverX. The technology involved in detecting cAMP levels is a no wash gain-of-signal competitive immunoassay based on Enzyme Fragment Complementation technology. Experiments were designed to test for either agonist or antagonist activity of the IgG clones. To test for agonist activity of the IgGs, cells were stimulated with IgG incubating for 30 min at 37°C (titrations 1:3 starting from 100 nM and diluting

down to 0.046 nM with PBS) or with the known agonist GLP-1 7–36 peptide (MedChemExpress, Cat. #HY-P005), titrated 1:3 starting from 12.5 nM with 12 points serial dilution with PBS. To test for antagonist activity, GLP1R-expressing cells (DiscoverX, Cat. #95-0062E2) are seeded at 15,000 cells per well. After overnight incubation, the cells were treated with titrated antibodies or antagonistic control Exendin 9–39 (AnaSpec Inc. AS-24467) for 1 hour at 37°C, followed by agonist stimulation of GLP-1 or Exendin-4 for 30 minutes at 37°C. cAMP level is evaluated one day after adding detection reagent.

Beta arrestin recruitment assay

β -arrestin recruitment assay was obtained from Eurofins DiscoverX (Cat #93-0300E2) that used untagged GLP-1 R-overexpressing CHO-K1 cells. This experiment tests whether TB01-3 has an effect on GLP-1 7–36 agonist-induced β -arrestin recruitment upon GLP-1 R activation. GLP1R-expressing cells (DiscoverX, Cat. #93-0300E2) are seeded at 10000 cells per well. After overnight incubation, the cells were treated with titrated antibodies for 1 hour at 37°C, followed by agonist stimulation of GLP-1 for 1 hour at 37°C. The level of β -arrestin is evaluated 3 hours after adding detection reagent by a Chemiluminescence plate reader (Molecular Devices SpectraMax M5) and output relative light unites were analyzed using GraphPad Prism.

Rat PK study

The rat PK study was performed at Charles River Laboratories (Worcester, MA).

5 male Sprague-Dawley rats as a group for each testing article were allowed to acclimate for a minimum of 3 days before dosing. TB01-3 and TB59-2 were dosed by intravenous infusion at 10 mg/kg in 100 mM Hepes, 100 mM NaCl, 50 mM sodium acetate, pH 6.0 vehicle. About 250 μ L blood samples were collected via jugular vein cannula at these time points: pre-dose, 0.0833, 0.25, 0.5, 1, 2, 4, 8, 24, 48, 72, 96, 168, 240 and 336 hours post dose. All blood samples were collected into K₂ EDTA tubes and processed to plasma by centrifugation at 3500 rpm for 10 minutes at 5°C within 30 minutes of collection. Plasma samples were then transferred into an appropriate tube containing DPP-4 (3.3 μ L for 100 μ L of plasma) and frozen on dry ice.

To measure the human IgG concentration in rat plasma samples using an ELISA, sheep anti-Human IgG (1 mg/mL) was used as coating reagent (The Binding Site, Lot No. AU003.M), and goat anti-Human IgG, HRP (H&L) (1 mg/mL) was used as detection reagent (Bethyl, cat #A80-319P). Stock solutions of human IgG standards and quality control samples (QCs) were prepared by spiking human IgG into rat plasma. A minimum of two wells were used to analyze each study samples, QCs, standards, and blank. A 4-parameter logistic (4PL) model was used to fit the sigmoid calibration curve. The semi-logarithmic sigmoid calibration curve was obtained by plotting the absorbance response against concentration. Concentrations of analyte in the test samples were determined by computer interpolation from the plot of the calibration curve.

In vivo PD studies

Animals

C57BL/6NHSd (Envigo RMS, LLC) male littermates at 8–10 weeks of age, weighing ~20–28 grams, were used in all the studies described. The

mice were housed in a room that was temperature (22–25 °C) and light-controlled (12-h: 12-h light/dark cycle starting at 7AM. The mice were fed with chow diet with 9% fat (PicoLab mouse Diet 20 (#5058), Lab Supply, Fortworth Texas, USA) for the duration of housing at the UCSF animal care facility.

Monoclonal Antibodies and Reagent

Anti-GLP-1 mAbs (an agonist mAb, TB59-2 and one antagonist mAb, TB01-3) in PBS buffer were tested in these studies. Mice were dosed prior to a GTT or an ITT using the following regimen: Agonist TB59-2 mAb was dosed at 5 or 10 mg/kg at three different administration regimen groups prior to performing a GTT and with four different administration regimen groups in an ITT, which were: 1) mAb administered as a single dose, 15 hours prior to GTT and 21 hours prior to ITT; 2) mAb administered as a double dose, 15 hours prior to GTT and 21 hours prior to ITT plus a second mAb dose 2 hours prior to GTT and ITT; 3) mAb single dose 2 hours prior to GTT and ITT; and 4) mAb single dose 6 hours prior to ITT only.

Antagonist TB01-3 mAb was dosed at 20 mg/kg at four different administration regimen groups: 1) mAb administered as a single dose, 15 hours prior to GTT and 21 hours prior to ITT; 2) mAb administered as a double dose, 15 hours prior to GTT and 21 hours prior to ITT plus a second mAb dose 2 hours prior to GTT and ITT; 3) mAb as a single dose 6 hours prior to GTT and ITT; and 4) mAb single dose 2 hours prior to GTT and ITT.

Extendin 9–39 Peptide (MedChemExpress, Cat. #HY-P0264) were dosed at 1.0 or 0.23 mg/kg at three different administration regimen groups: 1) Extendin administered as a single dose, 21 hours prior to ITT; 2) Extendin administered as a double dose, 21 hours prior to ITT plus a second Extendin dose 2 hours prior to ITT; and 3) mAb as a single dose 6 hours prior to ITT.

Glucose tolerance test

A GTT was used to assess the effects of two different anti-GLP1 mAbs (Agonist and Antagonist) on glucose tolerance following an acute glucose administration. An intraperitoneal (i.p.) GTT was conducted in 8- or 10-week-old male mice to assess glucose disposal after a glucose injection and measure blood glucose level after mice were fasted overnight (14–16 hours). To avoid circadian variations in mouse blood glucose levels, this testing was performed at fixed times. Mice were weighed after the overnight fast and baseline blood glucose levels (pre-glucose injection; Time 0 minutes) were measured. Mice were injected, i.p. with a single bolus (10 ul/gram body weight) of 30% dextrose solution (Hospira, Illinois) and blood glucose levels were measured at 15, 30, 60, 120 and 180 minutes post glucose administration. Blood samples were obtained by a tail nick and blood glucose levels were monitored using a OneTouch Ultra 2 glucose monitor (LifeScan, Inc.). Both ANOVA and t-tests were used to calculate the *p* values for the GTT assays, with the AUC analyzed by Ordinary One-Way ANOVA using GraphPad Prism 8.

Insulin tolerance test

An ITT was conducted to assess the effects of two different anti-GLP1 mAbs (agonist and antagonist) on insulin sensitivity following acute insulin administration. 8 or 10-week old male mice were fasted for 6 hours and body weight was recorded before and after fasting. To

avoid circadian variations in mouse blood glucose levels, this testing was performed at fixed times. Blood samples were collected by tail nick and baseline glucose was measured prior to insulin injection. Mice were injected (i.p.) with a single bolus (0.75 U/Kg body weight) of human insulin (Novolin, Novo Nordisk) and blood glucose levels were measured at 15, 30, 45, 60, and 120 minutes after insulin injection. Blood glucose levels were monitored using a OneTouch Ultra 2 glucose monitor (LifeScan, Inc.). Both ANOVA and t-tests were used to calculate the *p* values for the ITT assay using GraphPad Prism 8, with the AUC analyzed by Ordinary One-Way ANOVA.

Acknowledgments

The authors gratefully acknowledge the Distributed Bio and Twist Bioscience library team for their help in designing and synthesis of the GPCR focused library; and Catherine Hutchings for her critical review and constructive comments on this manuscript.

Abbreviations:

CDR, complementarity-determining region; GLP-1R, Glucagon-like peptide-1 receptor; GPCR, G protein-coupled receptor; NGS, next-generation sequencing; HI, hyperinsulinemia; GTT, glucose tolerance test; ITT, insulin tolerance test

Disclosure of Interest

This research is sponsored by Twist Bioscience and authors Qiang Liu, Pankaj Garg, Emily Tuscano, Linya Wang, Emily Sever, Erica Keane, Ana G Lujan Hernandez, Tom Yuan, Eric Kwan, Joyce Lai, Fumiko Axelrod, and Aaron K. Sato are employees of Twist Bioscience, a DNA synthesis and drug discovery service company.

References

1. Sriram K, Insel PA. G protein-coupled receptors as targets for approved drugs: how many targets and how many drugs? *Mol Pharmacol.* 2018;93(4):251–58. doi:10.1124/mol.117.111062.
2. Grigoriadis DE, Hoare SR, Lechner SM, Slee DH, Williams JA. Drugability of extracellular targets: discovery of small molecule drugs targeting allosteric, functional, and subunit-selective sites on GPCRs and ion channels. *Neuropsychopharmacology.* 2009;34(1):106–25. doi:10.1038/npp.2008.149.
3. Hauser AS, Attwood MM, Rask-Andersen M, Schiöth HB, Gloriam DE. Trends in GPCR drug discovery: new agents, targets and indications. *Nat Rev Drug Discov.* 2017;16(12):829–42. doi:10.1038/nrd.2017.178.
4. Lu RM, Hwang YC, Liu IJ, Lee CC, Tsai HZ, Li HJ, et al. Development of therapeutic antibodies for the treatment of diseases. *J Biomed Sci.* 2020;27:1.
5. Mullard A. FDA approves second GPCR-targeted antibody. *Nat Rev Drug Discov.* 2018;17:613.
6. Muratshahi E, Freissmuth M, Gruber CW. Nature-derived peptides: a growing niche for gpcr ligand discovery. *Trends Pharmacol Sci.* 2019;40(5):309–26. doi:10.1016/j.tips.2019.03.004.
7. Song G, Yang D, Wang Y, De Graaf C, Zhou Q, Jiang S, et al. Human GLP-1 receptor transmembrane domain structure in complex with allosteric modulators. *Nature.* 2017;546(7657):312–15. doi:10.1038/nature22378.
8. Nixon AE, Sexton DJ, Ladner RC. Drugs derived from phage display: from candidate identification to clinical practice. *MABS.* 2014;6(1):73–85. doi:10.4161/mabs.27240.
9. Mentlein R, Gallwitz B, Schmidt WE. Dipeptidyl-peptidase IV hydrolyses gastric inhibitory polypeptide, glucagon-like peptide-1 (7-36)amide, peptide histidine methionine and is responsible for their degradation in human serum. *Eur J Biochem.* 1993;214(3):829–35. doi:10.1111/j.1432-1033.1993.tb17986.x.

10. Todd JF, Bloom SR. Incretins and other peptides in the treatment of diabetes. *Diabet Med.* 2007;24(3):223–32. doi:10.1111/j.1464-5491.2006.02071.x.
11. Meier JJ, Nauck MA. The potential role of glucagon-like peptide 1 in diabetes. *Curr Opin Investig Drugs.* 2004;5:402–10.
12. Nauck MA, Meier JJ. MANAGEMENT OF ENDOCRINE DISEASE: are all GLP-1 agonists equal in the treatment of type 2 diabetes? *Eur J Endocrinol.* 2019;181(6):R211–r34. doi:10.1530/EJE-19-0566.
13. Uccellatore A, Genovese S, Dicembrini I, Mannucci E, Ceriello A. Comparison Review of Short-Acting and Long-Acting Glucagon-like Peptide-1 Receptor Agonists. *Diabetes Ther.* 2015;6(3):239–56. doi:10.1007/s13300-015-0127-x.
14. Rosenfeld E, Ganguly A, De Leon DD. Congenital hyperinsulinism disorders: genetic and clinical characteristics. *Am J Med Genet C Semin Med Genet.* 2019;181(4):682–92. doi:10.1002/ajmg.c.31737.
15. Vajravelu ME, De León DD. Genetic characteristics of patients with congenital hyperinsulinism. *Curr Opin Pediatr.* 2018;30(4):568–75. doi:10.1097/MOP.0000000000000645.
16. Larraufie P, Roberts GP, McGavigan AK, Kay RG, Li J, Leiter A, et al. Important Role of the GLP-1 Axis for Glucose Homeostasis after Bariatric Surgery. *Cell Rep.* 2019 Feb 5;26(6):1399–1408.e6.
17. Yorifuji T. Congenital hyperinsulinism: current status and future perspectives. *Ann Pediatr Endocrinol Metab.* 2014;19(2):57–68. doi:10.6065/apem.2014.19.2.57.
18. Boodhansingh KE, Kandasamy B, Mitteer L, Givler S, De Leon DD, Shyng S-L, Ganguly A, Stanley CA. Novel dominant K ATP channel mutations in infants with congenital hyperinsulinism: validation by in vitro expression studies and in vivo carrier phenotyping. *Am J Med Genet A.* 2019;179(11):2214–27. doi:10.1002/ajmg.a.61335.
19. Rahman SA, Nessa A, Hussain K. Molecular mechanisms of congenital hyperinsulinism. *J Mol Endocrinol.* 2015;54(2):R119–29. doi:10.1530/JME-15-0016.
20. Thomas P, Ye Y, Lightner E. Mutation of the pancreatic islet inward rectifier Kir6.2. Also Leads to Familial Persistent Hyperinsulinemic Hypoglycemia of Infancy *Hum Mol Genet.* 1996;5:1809–12.
21. Thomas PM, Cote GJ, Wohllk N, Haddad B, Mathew PM, Rabl W, et al. Mutations in the sulfonylurea receptor gene in familial persistent hyperinsulinemic hypoglycemia of infancy. *Science.* 1995;268(5209):426–29. doi:10.1126/science.7716548.
22. Seghers V, Nakazaki M, DeMayo F, Aguilar-Bryan L, Bryan J, Sur1 knockout mice. A model for K(ATP) channel-independent regulation of insulin secretion. *J Biol Chem* 2000; 275:9270–7.
23. Shimomura K, Maejima Y. K(ATP) Channel Mutations and Neonatal Diabetes. *Intern Med.* 2017;56:2387–93.
24. Meier JJ, Nauck MA. Is the diminished incretin effect in type 2 diabetes just an epi-phenomenon of impaired beta-cell function? *Diabetes.* 2010;59(5):1117–25. doi:10.2337/db09-1899.
25. De León DD, Li C, Delson MI, Matschinsky FM, Stanley CA, Stoffers DA. Exendin-(9-39) corrects fasting hypoglycemia in SUR-1^{-/-} mice by lowering cAMP in pancreatic beta-cells and inhibiting insulin secretion. *J Biol Chem.* 2008;283(38):25786–93. doi:10.1074/jbc.M804372200.
26. Göke R, Fehmann HC, Linn T, Schmidt H, Krause M, Eng J, et al. Exendin-4 is a high potency agonist and truncated exendin-(9-39)-amide an antagonist at the glucagon-like peptide 1-(7-36)-amide receptor of insulin-secreting beta-cells. *J Biol Chem.* 1993;268(26):19650–55. doi:10.1016/S0021-9258(19)36565-2.
27. De León DD, Deng S, Madani R, Ahima RS, Drucker DJ, Stoffers DA. Role of endogenous glucagon-like peptide-1 in islet regeneration after partial pancreatectomy. *Diabetes.* 2003;52(2):365–71. doi:10.2337/diabetes.52.2.365.
28. Calabria AC, Li C, Gallagher PR, Stanley CA, De León DD. GLP-1 receptor antagonist exendin-(9-39) elevates fasting blood glucose levels in congenital hyperinsulinism owing to inactivating mutations in the ATP-sensitive K⁺ channel. *Diabetes.* 2012;61(10):2585–91. doi:10.2337/db12-0166.
29. BARIATRIC NEWS. <https://investors.xoma.com/news-events/press-releases/detail/305/xoma-establishes-proof-of-concept-for-358-in-congenital>.
30. Ng CM, Tang F, Seeholzer SH, Zou Y, De León DD. Population pharmacokinetics of exendin-(9-39) and clinical dose selection in patients with congenital hyperinsulinism. *Br J Clin Pharmacol.* 2018;84(3):520–32. doi:10.1111/bcp.13463.
31. Pyke C, Heller RS, Kirk RK, Ørskov C, Reedtz-Runge S, Kaastrup P, Hvelplund A, Bardram L, Calatayud D, Knudsen LB, et al. GLP-1 receptor localization in monkey and human tissue: novel distribution revealed with extensively validated monoclonal antibody. *Endocrinology.* 2014;155(4):1280–90. doi:10.1210/en.2013-1934.
32. Jensen CB, Pyke C, Rasch MG, Dahl AB, Knudsen LB, Secher A. Characterization of the Glucagonlike Peptide-1 Receptor in Male Mouse Brain Using a Novel Antibody and In Situ Hybridization. *Endocrinology.* 2018;159(2):665–75. doi:10.1210/en.2017-00812.
33. Wu F, Yang L, Hang K, Laursen M, Wu L, Han GW, et al. Full-length human GLP-1 receptor structure without orthosteric ligands. *Nat Commun.* 2020;11(1):1272. doi:10.1038/s41467-020-14934-5.
34. DeWitt WS, Lindau P, Snyder TM, Sherwood AM, Vignali M, Carlson CS, et al. A public database of memory and naive b-cell receptor sequences. *PLoS One.* 2016;11(8):e0160853. doi:10.1371/journal.pone.0160853.
35. DeWire SM, Ahn S, Lefkowitz RJ, Shenoy SK. Beta-arrestins and cell signaling. *Annu Rev Physiol.* 2007;69(1):483–510. doi:10.1146/annurev.physiol.69.022405.154749.
36. Hutchings CJ, Koglin M, Olson WC, Marshall FH. Opportunities for therapeutic antibodies directed at G-protein-coupled receptors. *Nat Rev Drug Discov.* 2017;16:787–810.
37. Majima M, Ito Y, Hosono K, Amano H. CGRP/CGRP receptor antibodies: potential adverse effects due to blockade of neovascularization? *Trends Pharmacol Sci.* 2019;40(1):11–21. doi:10.1016/j.tips.2018.11.003.
38. Hutchings CJ. A review of antibody-based therapeutics targeting G protein-coupled receptors: an update. *Expert Opin Biol Ther.* 2020;20(8):925–35. doi:10.1080/14712598.2020.1745770.
39. Pan H, Su Y, Xie Y, Wang W, Qiu W, Chen W, et al. Everestmab, a novel long-acting GLP-1/anti GLP-1R nanobody fusion protein, exerts potent anti-diabetic effects. *Artif Cells Nanomed Biotechnol.* 2020;48(1):854–66. doi:10.1080/21691401.2020.1770268.
40. Camacho RC, You S, D’Aquino KE, Li W, Wang Y, Gunnet J, et al. Conjugation of a peptide to an antibody engineered with free cysteines dramatically improves half-life and activity. *MAbs.* 2020;12(1):1794687. doi:10.1080/19420862.2020.1794687.
41. Craig CM, Liu LF, Nguyen T, Price C, Bingham J, McLaughlin TL. Efficacy and pharmacokinetics of subcutaneous exendin (9-39) in patients with post-bariatric hypoglycaemia. *Diabetes Obes Metab.* 2018;20:352–61.
42. Liu T, Liu Y, Wang Y, Hull M, Schultz PG, Wang F. Rational design of CXCR4 specific antibodies with elongated CDRs. *J Am Chem Soc.* 2014;136:10557–60.
43. Zhang Y, Zou H, Wang Y, Caballero D, Gonzalez J, Chao E, et al. Rational design of a humanized glucagon-like peptide-1 receptor agonist antibody. *Angew Chem Int Ed Engl.* 2015;54:2126–30.